PHYSICAL REVIEW B VOLUME 42, NUMBER 9 15 SEPTEMBER 1990-II

Photoluminescence study of radiative channels in ion-implanted silicon

O. O. Awadelkarim, A. Henry, and B. Monemar
Department of Physics and Measurement Technology, University of Linköping, S-581 83 Linköping, Sweden

J. L. Lindström
National Defence Research Establishment, P.O. Box 1165, S-581 11 Linköping, Sweden

Y. Zhang and J. W. Corbett
Department of Physics, State University of New York, Albany, Albany, New York 12222
(Received 20 February 1990; revised manuscript received 1 June 1990)

Efficient radiative defects are introduced in boron-doped silicon by carbon- and oxygen-ion implantations and subsequent annealing up to 500 °C. They exhibit sharp and intense low-temperature photoluminescence transitions in a range between 767.0 meV (P line) and 1080.0 meV (Y line). From correlations between the line intensities and the oxygen and carbon contents in the samples, it is argued that the P center and the H center (925.4 meV) are carbon- and oxygen-related defects. The L line (1003.8 meV) is influenced by carbon, and it appears to be independent of oxygen. The X line (1040.0 meV) and the W line (1018.0 meV) are attributed to centers that are formed from intrinsic point defects. The generation and annealing of the G line (969.4 meV) and the C line (789.0 meV) in implanted Czochralski-grown material are reminescent of those in particle-irradiated silicon. However, for the G defect in implanted float-zone material, an alternative formation mechanism is proposed. Among the other observed photoluminescence lines, the two lines at 1101.4 and 1103.8 meV are reported here for the first time. The optical centers responsible for these two lines are tentatively suggested to involve oxygen and carbon.

I. INTRODUCTION

Ion implantation is indispensable in the fabrication of semiconductor devices of small dimensions, as in very-large-scale-integration (VLSI) technology. A necessary component of nearly all implantation processes is the exposure of semiconductor surfaces to bombardment with ions having energies of several kilo-electron-volts. The implantation of ions into semiconductors creates defects which can have a dramatic influence on the electrical and optical properties of the material. The defect structure is usually very complex compared to that present after electron or neutron irradiation. The complexity of the defect structures is often accentuated by changes in the implantation parameters, e.g., the ion mass, fluence, rate, and temperature of implantation. However, implanation of low fluences of light ions produces rather simple point defects. Quite a few of those seem to be common to both particle-irradiated and ion-implanted silicon.[1–3] The formation and annealing kinetics of some of these defects, although very well documented in the case of particle irradiation, are still under debate in ion-implanted silicon—partly because of the additional complications in the case of ion implantation brought about by factors such as the projection range, and diffusion of the implanted species and point defects into the undamaged substrate. This is to be contrasted with the case of particle irradiation where the damage is rather uniform throughout the material. Among the defects that are produced in particle-irradiated or ion-implanted silicon, are the so-called optical centers, which have been extensively studied using low-temperature photoluminescence (PL). Examples of these include the G center[4] and the C center,[5] as well as many other unidentified PL lines and bands.[1,6–8]

The current work was undertaken to study the formation and annealing properties of the photoluminescent centers in ion-implanted silicon. The implanted-ion species used are oxygen (O) and carbon (C). O implantations are frequently used for silicon-on-insulator (SOI) applications, whereas carbon is a common contaminant in layers formed by O implantation. A number of PL lines are observed. We shall give a brief survey of the spectral properties of these lines and discuss the identifications made in the light of sample treatments, as well as the defect-generation and annealing aspects. Defect-generation mechanisms in ion-implanted silicon are proposed for some of the observed luminescent centers. Aside from the previously observed PL lines, we also report on new PL lines detected in this study.

II. EXPERIMENTAL PROCEDURE

The samples used in this investigation were cut from ⟨100⟩ Czochralski-grown (CZ) and float-zone (FZ) boron-doped silicon wafers. The room-temperature resistivity of the CZ material is 15.2 Ω cm, whereas that of the FZ material is 0.6 Ω cm. The initial oxygen and carbon contents in the samples were determined from infrared (ir) measurements using the ASTM (American Society for Testing and Materials) method.[9] In CZ material the concentrations of oxygen and carbon were $\approx(1-2)\times10^{17}$ and $\approx4.0\times10^{16}$ cm^{-3}, respectively. In the FZ material,

 ©1990 The American Physical Society

however, both concentrations are below our detection limit ($\approx 10^{15}$ cm^{-3}).

Ion implantations with $^{12}C^+$, and $^{16}O^+$ ions were performed at nominal room temperature into the polished faces of the wafers. Ion doses of $\approx 1.0\times10^{15}$ cm^{-2} at 70, 80, 100, and 130 deV were used for C^+ and O^+ implantations corresponding to projected ranges for the implanted ions between 2000 Å (70 kev) and 3500 Å (130 keV). Double implantations with C and O were done first using C^+ at 80 keV, followed by O^+ at 100 keV, giving projected ranges of 2200 Å for both carbon and oxygen. The samples that are doubled implanted with C and O are hereafter referred to as $C^+ + O^+$-implanted samples for brevity. Subsequent isochronal annealing on the implanted samples was carried out in a diffusion furnace in air ambient with the samples placed in a quartz tube. The annealing temperatures were between 100 and 500 °C in steps of 100 °C, and the annealing time was 30 min.

The PL measurements were done at 2 K with the 6471-Å line of a Kr^+-ion laser for excitation. The luminescence was dispersed with a Spex Industries, Inc. 1404 0.85-m-focal-length double-grating monochromator fitted with two 600-grooves/mm gratings blazed at 1.6 μm. A liquid-nitrogen-cooled North Coast EO-817 Ge detector was used with a lock-in technique and spike-suppression electronics.[10] The spectral resolution is about 0.4 meV.

III. EXPERIMENTAL RESULTS

A. $C^+ + O^+$ implantations

Typical PL spectra at 2 K of CZ samples taken before implantation, directly after $C^+ + O^+$ implantation and annealing at 200 °C, are shown in Figs. 1(a), Fig. 1(b), and Fig. 1(c), respectively. All spectra contained the phonon replica of the boron bound exciton (BE), a weak no-phonon transition (B^{NP}), the transverse-acoustic transition (B^{TA}), the transverse-optical transition (B^{TO}), the two-phonon-replica transition ($B^{TO} + O^{\Gamma}$), as well as the two-hole transition ($B^{TO} + B_h$) of the boron BE. In the spectra taken in the implanted or annealed samples in Figs. 1(b) and 1(c), other BE lines, such as the *W* line (1018.0 meV), the *G* line (969.4 meV), and the *C* line (789.0 meV) are seen. These lines were not present in the unimplanted samples, being CZ or FZ. Apart from differences in the line intensities, the unimplanted CZ and FZ material gave PL spectra similar to that shown in Fig. 1(a). In Fig. 2 the spectra obtained on the $C^+ + O^+$-implanted CZ samples after subsequent annealing at 300, 400, and 500 °C are shown. The *G* line has disappeared following annealing at 200 °C, whereas the *C* and *W* lines persisted until after annealing at 400 °C. Upon annealing the CZ material at temperatures ≥ 300°C, other PL lines are observed. These include (i) the *P* line (767.0 meV), (ii) the *X* line (1040.0 meV), (iii) the *L* line (1003.8 meV), (iv) the *H* line (925.4 meV), and (v) a line at 950.0 meV previously observed by Johnson and Compton.[11] Except for the *G* line the notation for the PL lines used here is taken from Tkachev and Mudryi.[1] Some weaker lines also occur at different annealing stages located at 856.0, 919.8 (the *N* line), 1099.4, 1101.4, and 1103.8 meV. The latter three lines, together with B^{TA} and lines associated with boron bound-multiexciton complexes (BMEC's),[12] being

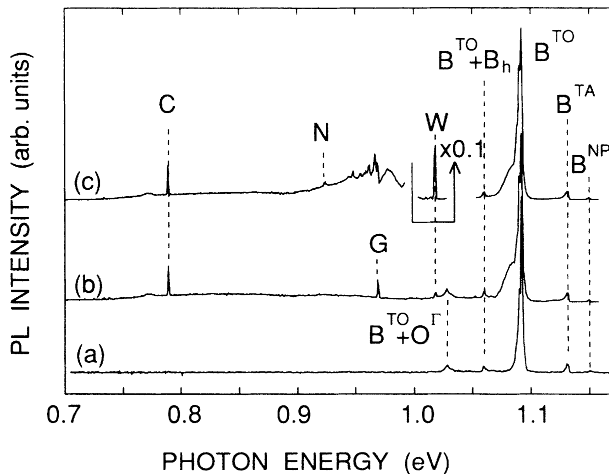

FIG. 1. Luminescence spectra from ($C^+ + O^+$)-implanted CZ samples (a) directly after implantation and (b) following implantation and (c) annealed at 200 °C. B^{NP}, B^{TA}, and B^{TO} are the no-phonon, the transverse-acoustic, and the transverse-optical phonon replicas of the boron bound exciton, respectively. $B^{TO} + B_h$ and $B^{TO} + O^{\Gamma}$ are, respectively, the two-hole transition and the two-phonon replica of the boron bound exciton. The *W*-line intensity shown in the figure is one-tenth its observed value.

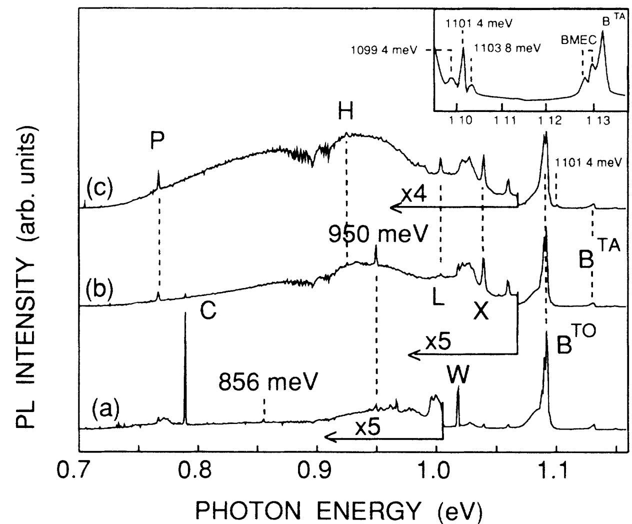

FIG. 2. Photoluminescence spectra taken in $C^+ + O^+$-implanted CZ material after annealing at (a) 300 °C, (b) 400 °C, and (c) 500 °C. In the spectra only the transverse-optical (B^{TO}) and transverse-acoustic (B^{TA}) phonon replicas of the boron bound exciton are labeled together with the defect-related bound-exciton lines. The spectrum shown in the inset of the figure is magnified 10 times and it shows the weak transitions at 1099.4, 1101.4, and 1103.8 meV as well as B^{TA} and lines associated with boron bound-multiexciton complexes (BMEC's). The parts of the spectra indicated by the arrows are magnified by the factors specified in the figure, and the structure around 0.9 eV is due to water absorption.

weak, are highlighted in the inset of Fig. 2. The energy position, 1099.4 meV, is close to that estimated for the longitudinal-optical-phonon replica of the free exciton (FE^{LO}),[12,13] whereas the lines at 1101.4 and 1103.8 meV were not previously reported in any similar PL studies.

In order to study the annealing characteristics of the observed PL lines, the excitation power was kept constant and the PL intensities of the lines were measured relative to the intensity of B^{TO}, which was assumed to stay constant during the annealing. Such an assumption is reasonable to make since most of the luminescence from the boron BE is expected to come from the unimplanted substrate, where the concentrations of boron and other recombination channels are, presumably, constant. The annealing properties of the observed PL lines are depicted in Fig. 3(a). The PL intensity of the *W* line increases with increasing annealing at 200 °C, when it completely dominates the PL spectrum of the sample. The *W* line disappears following annealing at 500 °C. The intensity of the *G* line decreases with annealing and it is not detectable in the samples upon annealing at 200 °C. The *C* line, on the other hand, is annealed out at 500 °C. The *X* and *P* lines, after being introduced upon annealing at 300 °C, increased in intensity as the annealing temperature was elevated to 500 °C. The 1101.5-meV and the *L*-line are produced following annealing at 400 and 500 °C. The 1103.8-meV line is only seen after annealing at 500 °C.

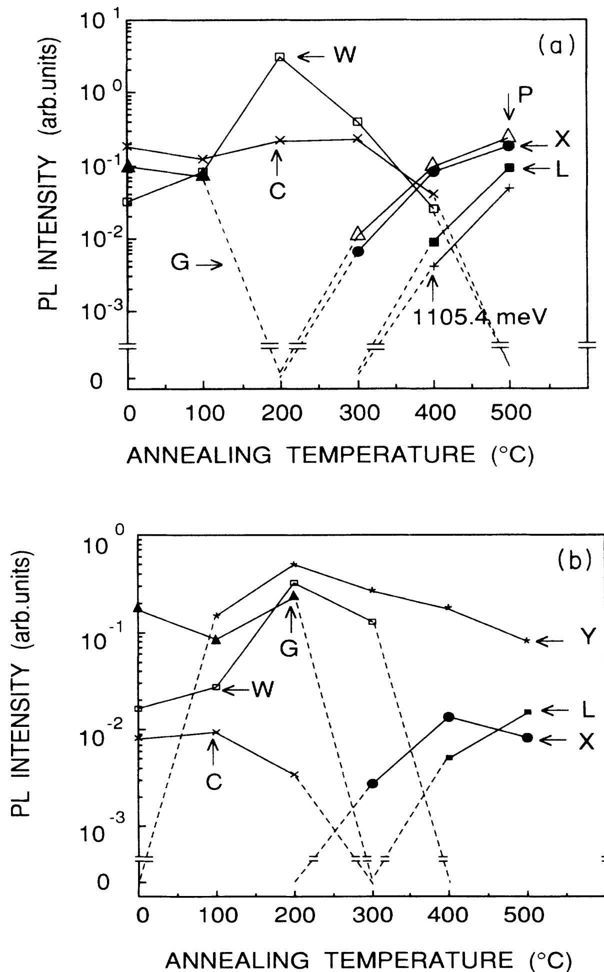

FIG. 3. Points show experimental data for the photoluminescence line intensity relative to the intensity of the transverse-optical (B^{TO}) replica of the boron bound exciton as a function of the annealing temperature (a) ($C^+ + O^+$)-implanted CZ samples, and (b) C^+-implanted FZ samples. The annealing time is 30 min.

In the FZ material the *W* and *X* lines appeared at intensities comparable to those in the CZ material. They also exhibited annealing properties similar to the CZ samples. None of the other PL lines described above were detectable in the similarly treated FZ samples. However, an additional PL transition at 1080.0 meV (*Y* line) is seen only in implanted FZ material following annealing at 100 °C.

B. C^+ implantation

Representative PL spectra recorded in C^+-implanted FZ material are shown in Fig. 4. In the spectra, we label the *Y*, *X*, *W*, *G*, and *C* lines, as well as the *L* line, which appears in relatively weaker intensities in the annealing temperature range 300–500 °C. All lines showed annealing characteristics very similar to those described in the preceding subsection [Fig. 3(b)]. Similar PL behavior is measured in the C^+-implanted CZ material, except for the *Y* line, which is not seen in this material.

C. O^+ implantations

In O^+-implanted FZ material only the *W* line, the *X* line, and the *Y* line are seen at different annealing stages, similar to those described in the preceding subsections. A survey spectrum of the *W* line was, however, possible to obtain in this sample due to the absence of many strong nearby transitions that normally appear in samples implanted with C^+ and $C^+ + O^+$. Such a spectrum is shown in Fig. 5, exhibiting fivefold vibronic structures

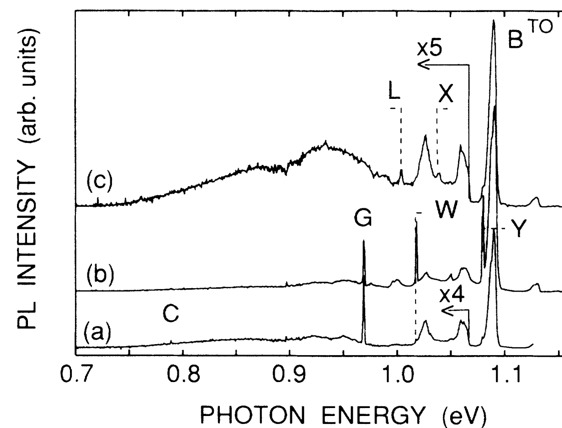

FIG. 4. Luminescence spectra recorded in C^+-implanted FZ samples (a) directly after implantation, and following annealing at (b) 200 °C and (c) 500 °C. The parts of the spectra indicated by the arrows are magnified by the factors specified in the figure.

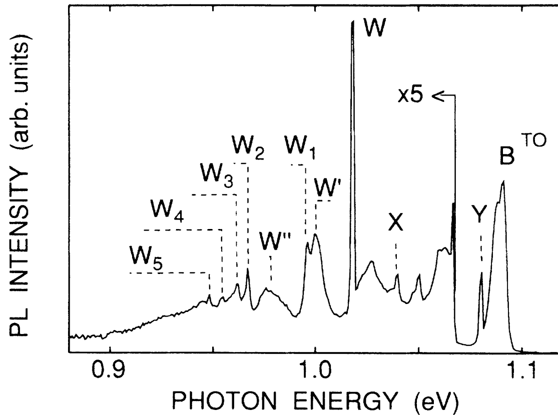

FIG. 5. Luminescence spectrum centered at the NP W line taken in O^+-implanted FZ sample annealed at 200 °C. The side-band structure ($W_1 \cdots W_5, W', W''$) of the W emission is labeled in the figure. The part of the spectrum to the left of the arrow is magnified by the specified factor.

which accompany the no-phonon transition of the W line. As shown in the figure, the detailed shape of the W band comprises $W_1 \approx 996.8$ meV, $W_2 \approx 967.4$ meV, $W_3 \approx 962.4$ meV, $W_4 \approx 955.0$ meV, and $W_5 \approx 948.8$ meV, together with broad peaks labeled W' and W'' on the lower-energy side of the zero-phonon line W. These assignments are made in comparison with data on the W band reported in Ref. 1.

As described above, the Y line is observed in the annealed FZ samples irrespective of the implanted-ion species. This transition was originally reported by Noonan *et al.*,[14] but seen only after boron implantations in all material irrespective of the growth method. Interestingly, we were able to detect the Y line in silicon implanted with atoms other than boron, however only in highly-boron-doped samples. Boron-isotope-effect studies have revealed the presence of two boron atoms in the defect.[15,16] No substantial annealing is observed in the Y line up to tempertures as high as 500 °C [Fig. 3(b)].

IV. DISCUSSION

A. The *W* and *X* lines

The W and X lines are consistently observed in all the samples irrespective of their growth methods or the implanted-ion species. Within permissible experimental errors, the introduction of these lines, their annealing behaviors, and intensities in all of the samples are somewhat similar [Figs. 3(a) and 3(b)]. These observations indicate that the defect centers giving rise to the W and X lines include neither oxygen nor carbon. It is plausible to associate these lines with centers comprising intrinsic point defects, e.g., vacancies and self-interstitials, resulting from atomic displacements caused by interactions with the energetic ions.

The W line and the X line are frequently observed in neutron-irradiated,[1] ion-implanted,[17] or laser-annealed ion-implanted silicon.[18] They are insensitive to carbon-isotope substitution,[19] and they are not dependent on the presence of any other impurity in the crystal.[1] The local-mode vibrational frequency of the W line seen in luminescence shows isotope effects consistent with vibrations from only silicon atoms.[20] The application of a magnetic field introduces no detectable change in the W line, suggesting that it arises from interactions between spinless states.[19,20] Furthermore, uniaxial-stress perturbations introduce no resolvable splittings on the W line—only a rather small energy shift in the line position—and broadening has been observed at a stress of about 80 kg mm^{-2}.[1]

It has been suggested that the W line arises from a defect involving five vacancies,[1] i.e., the same defect that is proposed to be responsible for the electron-paramagnetic-resonance (EPR) spectrum labeled Si-$P1$.[21] The X line, on the other hand, is ascribed to the trivacancy complex.[1] According to these identifications, the growth in the concentration of the X center [Figs. 3(a) and 3(b)] upon annealing at temperatures ≥ 300 °C may be explained as being due to the disintegration of the W defect, hence supplying the vacancies that are necessary for the formation of the X center.

B. The *G* and *C* lines

The G line is one of the most extensively studied PL lines in silicon.[1,17,22] The model of the G center appears to be firmly established from the simultaneous application of different techniques. The annealing properties and the uniaxial-stress splitting of the G NP line had suggested the association of the defect to the EPR $G11$ center that comprises two carbon atoms occupying a substitutional lattice site.[4,23,24] The involvement of carbon in the center was later verified by the isotope shifts in the NP line as well as in the vibrational side bands.[23,25]

Optically-detected-magnetic-resonance (ODMR) experiments then revealed that a nonradiative excited spin-triplet state correlates with the G line.[26] Based on the ODMR data, a C_s-Si_i-C_s (subscripts s and i stand for substitutional and interstitial, respectively) structure has been proposed for the G center. In this configuration the center is of C_{3v} symmetry. In contrast, the G optical emission is a singlet-to-singlet transition. However, a second relevant structure for the G center in its positive and negative charge states has been deduced from EPR measurements.[24,27,28] In this latter structure, the split-interstitial configuration C_iC_s is preserved and the center's symmetry is C_{1h}. The two structural forms of the G center exhibit configurational bistability.[28]

The PL spectrum of oxygen-rich irradiated silicon often contains a NP transition at 790 meV, commonly labeled the C line.[22,29,30] Isotope-substitution experiments show that the center contains one carbon atom and one oxygen atom.[5,31] This center is also observed in EPR as $G15$, in its singly positive charge state,[32] and modeled as a C_iO_i pair possessing monoclinic $I\ C_{1h}$ symmetry.[33]

The annealing behaviors observed here for the G and C lines are similar to those in electron- or neutron-irradiated CZ material (c.f., Ref. 1). This indicates that

the mechanisms responsible for the formations of the G and C centers in implanted CZ samples are the same as in irradiated CZ material. However, in implanted FZ samples the C and G lines are only observed following C^+ implantations (Fig. 4), and the lines are absent in the O^+- or $C^+ + O^+$-implanted FZ samples. It is also noted that the G line in both CZ and FZ samples appears at high intensities, whereas the intensity of the C line in FZ material is significantly low. This latter observation is obviously due to the oxygen content being very low in the FZ samples used. However, the formation of the G center in the FZ material can be viewed as being due to two of the implanted carbon atoms sharing a vacant lattice site left behind by a displaced silicon atom. The displaced silicon atom resides interstitially nearby the CC pair, thus, allowing for the Si-C interstitialcy in the luminescent C_s-Si_i-C_s structure of the G center. This formation model is to be contrasted with other models in which the G center is proposed to be formed as a result of a static substitutional carbon atom, originally present in the crystal lattice, trapping a mobile interstitial carbon atom during different treatments, such as electron irradiation or reactive-ion etching.[34] However, the absence of the G and C lines in the FZ material implanted with $C^+ + O^+$, and O^+ ions indicates that the presence of oxygen results in more complex defect-formation patterns.

C. The *P* and *H* lines

Heat treatment of CZ silicon at $\approx 450\,^{\circ}C$ for several hours produces the P line and the H line.[35–37] Their properties are typical of radiative transitions at deep neutral levels,[38] i.e., sharp and very intense NP lines, with a series of sharp satellites involving local vibrational modes.

In the results presented here, the P center is produced only in implanted CZ material (Fig. 2). However, it is present after relatively short (30 min) heat treatment at temperature as low as 300 °C. These results are to be compared with previously published data on this center in thermally treated CZ silicon,[36,37] which we may summarize as follows: (i) the center is produced following annealing at tempertures $\geq 400\,^{\circ}C$, (ii) it requires several hours of annealing at these tempertures for its formation, and (iii) it attains a maximum PL intensity after annealing at 450 °C and decreases in intensity upon annealing above this temperature. According to our data, the P center grows in concentration as the annealing temperature is raised to 500 °C. It is also more intense in the $C^+ + O^+$-implanted material, in comparison to the C^+- or O^+-implanted samples. Furthermore, the P center is completely absent in similarly treated FZ material. It is therefore inferred from the results that the P center contains both oxygen and carbon in its formation. The enhanced generation of the P center in the implanted material after short-duration and relatively-low-temperature annealing is hence attributed to the presence of abundant oxygen and carbon as the result of implantations. The involvement of oxygen in the P center has been suggested earlier in numerous PL studies.[1,37,39] The formation kinetics of the P center have features resembling those of the 450-°C thermal donors.[37,40] Nevertheless, no simple relationship between the thermal donors and the P defect could be deduced. As for the carbon involvement in the P center, an asymmetric line broadening, possibly indicating an unresolved splitting, has been observed in ^{13}C-enriched silicon, and has tentatively been ascribed to the carbon-isotope effect.[31] Arguments similar to the above imply that the H defect may also be oxygen and carbon related.

D. The *N* and *L* lines

The L line is detected after annealing at 400 °C and increases in intensity upon annealing at 500 °C. However, the interesting observation regarding the L line is its occurrence, although weak, in the implanted FZ material. The L line in the FZ material is only observed in C^+-implanted samples, and it is not seen in the $(C^+ + O^+)$- or O^+-implanted samples. These observations are new and cast doubts on earlier suggestions that the L center may be oxygen related.[1] The L line has previously been observed, but only in neutron-irradiated CZ silicon. This has led to the tentative association of the L center with either the trivacancy-trioxygen or the trivacancy-dioxygen center.[1] Our results, on the contrary, suggest that the center is independent of oxygen and could be carbon related. Data on carbon-isotope effects are necessary for the confirmation of the carbon involvement in the center.

The N line has been previously observed in electron- and neutron-irradiated CZ-grown silicon upon annealing between 300 and 450 °C.[1,31] To the best of our knowledge, this is the first time that the N line has been reported in ion-implanted silicon at low annealing tempertures of 200 °C. ^{13}C- and ^{14}C-isotope shifts establish that carbon is a constituent of the N center.[31]

E. The 1101.4- and 1103.8-meV transitions

The 1101.4-meV line is detected after annealing at 400 °C, and it increases in intensity as the annealing temperature is raised to 500 °C [Fig. 3(a)]. The 1103.8-meV line is observed upon annealing at 500 °C. These lines are only observed in CZ material doubly implanted with both oxygen and carbon (inset of Fig. 2), or implanted with carbon alone. This is suggestive of the necessity for abundant oxygen and carbon in the generation of the corresponding defects. These PL lines are reported here for the first time, and more work is still in progress to reveal information on the defect identities.

V. CONCLUSIONS

In summary, we have performed a low-temperature photoluminescence study of optical defects introduced by ion implantations (C^+ and O^+) in CZ and FZ boron-doped silicon. The conclusions from this study are the following.

The two centers responsible for the W line (1018.0 meV) and the X line (1040.0 meV) are consistently observed in all the samples, irrespective of their growth

methods or the implanted-ion species. Our data on the annealing characteristics and intensities of these lines suggest that they arise from centers involving intrinsic point defects. In the implanted CZ material the generation and annealing of the *G* line (969.4 meV) and the *C* line (789.0 meV) are similar to those in particle-irradiated silicon. However, in implanted FZ samples the formation of the *G* center is proposed to occur as a result of two implanted carbon atoms sharing a vacant substitutional lattice site left behind by a displaced silicon atom.

The occurrences of the *P* line (767.0 meV) and the *H* line (925.4 meV) in the samples suggest that the carbon and oxygen atoms are among the constituents of the corresponding defects. The *L* center (the *L* line at 1003.8 meV) is shown to be independent of oxygen, contrary to previous propositions that the center may be oxygen related. At present, in the absence of ^{13}C and ^{18}O data, these findings cannot be unambiguously confirmed. Nonetheless, this is the first time that the *L* line has been seen in ion-implanted silicon.

New PL emissions at 1101.4 and 1103.8 meV are detected in the samples. These lines are only observed in carbon or in carbon and oxygen double-implanted CZ samples after heat treatments at 400 and 500 °C. It is possible that both centers contain oxygen and carbon in their structures. More detailed studies are needed to identify the structure of these defects. Such work is in progress.

[1]V. D. Tkachev and A. V. Mudryi, in *Radiation Effects in Semiconductors 1976,* Inst. Phys. Conf. Ser. No. 31, edited by N. B. Urli and J. W. Corbett (IOP, Bristol, 1977), p. 231.

[2]H. J. Stein, in *Defects in Electronic Materials,* Vol. 104 of *Materials Research Society Symposia Proceedings,* edited by M. Stabola, S. J. Pearton, and G. Davies (MRS., Pittsburgh, 1988), p. 173.

[3]H. J. Stein, in *Defects in Semiconductors,* Vols. 10–12 of Materials Science Forum, edited by H. J. von Bardeleben (Trans Tech, Aedermannsdorff, Switz., 1986), p. 935.

[4]K. P. O'Donnell, K. M. Lee, and G. D. Watkins, Physica B + C (Amsterdam) **116B**, 258 (1983).

[5]K. Thonke, G. D Watkins, and R. Sauer, Solid State Commun. **51**, 127 (1984).

[6]J. Weber and M. Singh, Appl. Phys. Lett. **49**, 1617 (1986).

[7]J. I. Pankove and C. P. Wu, Appl. Phys. Lett. **35**, 937 (1979).

[8]R. A. Street, N. M. Johnson, and J. F. Gibbons, J. Appl. Phys. **50**, 8201 (1979).

[9]*Annual Book of ASTM Standards* (ASTM, Philadelphia, 1981), procedure F120, pp. 543–547.

[10]A. T. Collins and T. Jeffries, J. Phys. E **15**, 712 (1982).

[11]E. S. Johnson and W. D Compton, in *Radiation Effects in Semiconductors,* edited by J. W. Corbett and G. D. Watkins (Gordon and Breach, London, 1971), p. 219.

[12]P. McL. Colley and E. C. Lightowlers, Semicond. Sci. Technol. **2**, 157 (1987).

[13]M. A. Vouk and E. C Lightowlers, J. Lumin. **15**, 357 (1977).

[14]J. R. Noonan, C. G. Kirkpatrick, and B. G. Streetman, Radiat. Eff. **21**, 225 (1974).

[15]E. Irion, K. Thonke, and R. Sauer, J. Phys. C **18**, 5069 (1985).

[16]G. Davies, Phys. Rep. **176**, (1989).

[17]C. G. Kirkpatrick, J. R. Noonan, and B. G. Streetman, Radiat. Eff. **30**, 97 (1981).

[18]M. S. Skolnick, A. G. Collis, and H. C. Webber, J. Lumin. **24/25**, 39 (1981).

[19]N. Burger, K. Thonke, and R. Sauer, Phys. Rev. Lett. **52**, 1645 (1984).

[20]G. Davies, E. C. Lightowlers, and Z. E. Ciechanowska, J. Phys. C **20**, 191 (1987).

[21]Y. H. Lee and J. W. Corbett, Phys. Rev. B **8**, 2810 (1973).

[22]R. J. Spry and W. D. Compton, Phys. Rev. **17**, 1010 (1968).

[23]K. Thonke, H. Klemisch, J. Weber, and R. Sauer, Phys. Rev. B **24**, 5874 (1981).

[24]K. L. Brower, Phys. Rev. B **9**, 2607 (1974).

[25]G. Davies and M. C. do Carmo, J. Phys. C **14**, L687 (1981).

[26]K. M. Lee, K. P. O'Donnell, J. Weber, B. C. Cavenett, and G. D. Watkins, Phys. Rev. Lett. **48**, 37 (1982).

[27]K. L. Brower, Phys. Rev. B **17**, 4130 (1978).

[28]L. W. Song, X. D. Zhan, B. W. Benson, and G. D. Watkins, Phys. Rev. Lett. **60**, 460 (1988).

[29]A. P. Hare, G. Davies, and T. A. Collins, J. Phys. C **5**, 1265 (1972).

[30]J. Wagner, K. Thonke, and R. Sauer, Phys. Rev. B **29**, 7051 (1984).

[31]G. Davies, E. C. Lightowlers, R. A. Wooley, R. C. Newman, and A. C. Oates, J. Phys. C **17**, L499 (1984).

[32]Y. H. Lee, J. W. Corbett, and K. L. Brower, Phys. Status Solidi A **95**, 673 (1977).

[33]J. M. Trombetta and G. D. Watkins, Appl. Phys. Lett. **51**, 1103 (1987).

[34]J. Weber, R. J. Davis, H. -U. Habermeier, W. D. Sawyer, and M. Singh, Appl. Phys. A **41** (1986).

[35]N. S. Minaev and A. V. Mudryi, Phys. Status Solidi A **68**, 561 (1981).

[36]J. Weber and R. Sauer, in *Defects in Semiconductors II,* Vol. 14 of *Materials Research Society Symposia Proceedings,* edited by S. Mahajan and J. W. Corbett (Elsevier, Amsterdam, 1983), p. 165.

[37]N. Magnea, A. Lazrak, and J. L. Pautrat, Appl. Phys. Lett. **45**, 60 (1984).

[38]R. Sauer and J. Weber, Physica B + C (Amsterdam) **116B**, 195 (1983).

[39]J. Wagner, A. Dörnen, and R. Sauer, Phys. Rev. B **31**, 5561 (1985).

[40]M. Tajima, P. Stallhofer, and D. Huber, Jpn. J. Appl. Phys. Pt. 2, **22**, L586 (1983).